New Polyaniline Derivatives: Poly(4,4′-diphenylamine methylenes) and Poly(4,4′-diphenylimine methines)

Wen-Chang Chen and Samson A. Jenekhe*

Department of Chemical Engineering and Center for Photoinduced Charge Transfer, University of Rochester, Rochester, New York 14627-0166

Received March 30, 1992

ABSTRACT: New polyaniline derivatives consisting of alternating *p*-phenylene rings and nitrogen and carbon atoms in the backbone are prepared and characterized as model systems for the study of the role of the nitrogen atom on the structure and electronic and optical properties of polyanilines. The new polymers, poly(4,4′-diphenylamine methylenes) and poly(4,4′-diphenylimine methines), are analogues of and isoelectronic with leucoemeraldine and pernigraniline oxidation states of polyaniline, respectively. The substitution of an amine nitrogen atom of polyleucoemeraldine with a methylene carbon atom results in an increase of the π–π^* optical band gap. The substitution of an imine nitrogen atom of polypernigraniline with a methine carbon atom results in a significant reduction of the oscillator strength of the π–π^* absorption band near 2.2 eV. This optical band gap in the electronic spectra of the poly(4,4′-diphenylimine methines) varies from 540 nm (2.3 eV) to 687 nm (1.8 eV) depending on the side-group substitution at the methine carbon atom. One of the poly(4,4′-diphenylimine methines), **4d**, was found to exhibit a very dramatic solvatochromism: it is red in DMF or NMP (λ_{max} = 488 nm) and dark blue in THF (λ_{max} = 639 nm). The solvatochromism of these polyaniline derivatives is explained by conformational changes due to solvent quality. The new polyaniline derivatives are promising model systems for the experimental and theoretical understanding of the electronic structure and physical properties of polyanilines and other ring-containing conjugated polymers.

Introduction

Among conjugated polymers of current interest as electronic, electrochemical, and nonlinear optical materials,[1,2] polyaniline has probably attracted the greatest recent interest because of its relatively good environmental stability and the control of the electronic and optical properties by the level of oxidation and protonation.[3] Conductive polyaniline is currently used as active electrodes in commercial batteries and has been proposed for other applications, including electrochromic windows.[4,5] Recently, the various forms of polyaniline and its derivatives were reported to have interesting nonlinear optical properties.[6]

The unique features of electroactive polyaniline arise from the structural variations made possible by the alternating *p*-phenylene ring and nitrogen atom in the polymer backbone. Thus, the degree of oxidation can be varied by varying the fraction of the nitrogen atoms that is imine (=N–, sp^2) or amine (>N–, sp^3), as shown by the two extreme cases (**1** and **2**) in Chart I. Polyleucoemeraldine base (**1**, PLEMB), polyemeraldine base (PEMB), and polypernigraniline base (**2**, PPGN) with 0, 50, and 100% degree of oxidation, respectively, are the most widely studied forms of polyaniline. Each oxidation state of polyaniline has been found to exhibit dramatically different electronic properties. Polyemeraldine base can be protonated to give the highly conductive material (~1–20 S/cm)[7–9] whereas neither polyleucoemeraldine base nor polypernigraniline base becomes highly conducting on protonation.[10] Similarly, our group recently found that the third-order nonlinear optical susceptibility $\chi^{(3)}(-3\omega;\omega,\omega,\omega)$ of the polyanilines, measured by picosecond third harmonic generation spectroscopy in the wavelength range 0.9–2.4 μm, strongly depends on the degree of oxidation.[6] Polyemeraldine base was found to have the largest third-order nonlinear optical response among the different forms of polyaniline.[6b]

The nature of the bridge nitrogen atom (sp^2 or sp^3) is also of central importance in the theoretical understanding of the electronic and optical properties of polyaniline. The strong admixture of nitrogen p_z orbitals with the π orbitals of the phenylene ring causes a significant effect on the electronic band structures of polyaniline.[11–13] Polyleucoemeraldine base has been calculated to have a band gap of 3.8 eV, which is reasonably close to the experimental value (about 3.3 eV).[11] Polypernigraniline base with the all-sp^2 nitrogens has a degenerate ground-state structure and hence has been predicted to exhibit nonlinear soliton excitations with fractional charge.[13] In the doped state of polypernigraniline, a polaron is the most stable excitation.

Structural variation of the polyanilines has also been achieved by methods other than the degree of oxidation. Polyaniline with alkyl,[14,15] aryl,[16] sulfonic acid,[17] and alkoxy[6b] substituents on the benzene ring and alkyl,[18] benzyl,[19] and aryl[20] substituents on the nitrogen atom have been prepared and investigated. Random copolymers of polyanilines have also been prepared in our laboratory. Although substitutents on the benzene ring or nitrogen atom can significantly improve the solubility of polyaniline, they can also cause strong steric hindrances with adverse effects on the physical properties. In fact, most of the substituted polyanilines reported to date have inferior

Chart I

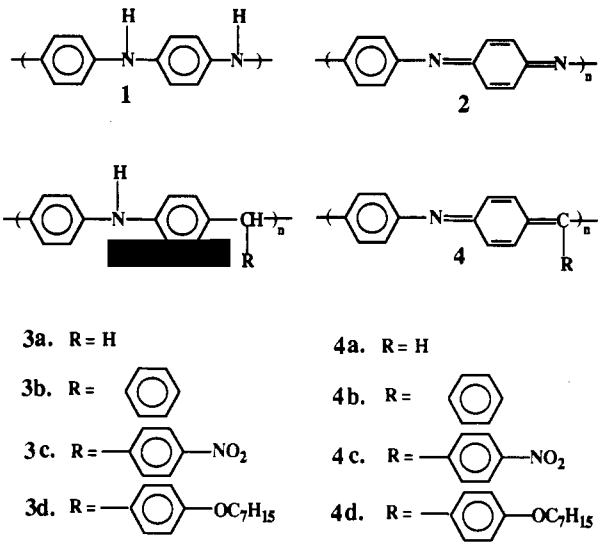

0024-9297/92/2225-5919$03.00/0

electrical and optical properties when compared with the parent polyaniline.

In this paper, we report the preparation and characterization of a new class of polyaniline derivatives consisting of alternating *p*-phenylene rings and nitrogen and carbon atoms. Such a novel class of polyanilines is of interest as model systems for the investigation of the effect of the nitrogen atom on the structure and properties of the polyanilines. By substituting a carbon atom for one of the two nitrogen atoms in the repeat units of polyleucoemeraldine base and polypernigraniline base, we obtain poly(4,4′-diphenylamine methylene) (**3a**, PDPAM) and poly(4,4′-diphenylimine methine) (**4a**, PDPIM), respectively, which are *isoelectronic* with the parent *all-nitrogen* polyanilines (**1** and **2**). The new polyaniline derivatives (**3** and **4**) will also allow investigation of the effect of intramolecular charge transfer on the electronic and optical properties of polyanilines through donor or acceptor substituents (R in Chart I) at the bridge carbon. The poly(4,4′-diphenylamine methylenes) (**3a–d**) were synthesized by acid-catalyzed polymerization of diphenylamine with aldehydes. The poly(4,4′-diphenylimine methines) (**4a–d**) were obtained from the corresponding poly(4,4′-diphenylamine methylenes) by dehydrogenation with 2,3-dichloro-5,6-dicyano-1,4-benzoquinone (DDQ). The nonlinear optical properties of some of the new polyaniline derivatives have been measured by picosecond third harmonic generation spectroscopy and will be reported in a separate paper.

Experimental Section

Materials. Diphenylamine (99+%, Aldrich), 2,3-dichloro-5,6-dicyano-1,4-benzoquinone (99+%, Aldrich), paraformaldehyde (Kodak), *p*-dioxane (Fisher), 1-methyl-2-pyrrolidinone (NMP; 99+% anhydrous, Aldrich), tetrahydrofuran (99.9%, anhydrous, Aldrich), and *p*-nitrobenzaldehyde (99.5%, Aldrich) were used without further purification. *p*-(Heptyloxy)benzaldehyde (98%, Chemical Dynamics) and benzaldehyde (99+%, Aldrich) were purified by vacuum distillation.

Synthesis of Polymers. Poly(4,4′-diphenylamine methylene) (PDPAM, 3a). The reaction mixture was 10 g of diphenylamine, 1.77 g of paraformaldehyde, 40 mL of *p*-dioxane, and 1.07 mL of 96% concentrated sulfuric acid. The reaction was maintained at 85 °C for 2 h. A yellowish-brown reaction mixture was precipitated in 700 mL of stirring methanol, recovered, extracted by methanol and then acetone in a Soxhlet apparatus for 12 h, and dried in a vacuum oven at 70 °C for 12 h. The product was a slightly brown powder (70% yield). Anal. Calcd for $[(C_{13}H_{11}N)_{0.98}(C_{13}H_{12}NSO_4)_{0.02}]_n$: C, 85.25; H, 6.04; N, 7.64. Found: C, 85.26; H, 6.01; N, 7.26. IR (film on NaCl, cm^{-1}): 3394, 3029, 2900, 2837, 1597, 1512, 1435, 1393, 1367, 1310, 1225, 1177, 1133, 809, 747, 693, 621. UV–vis (λ_{max}, NMP): 298 nm (log ϵ = 4.04). ^{1}H NMR (δ, ppm, referenced to TMS, soluble fraction in DMSO-d_6): 3.71 (2 H, CH_2), 4.88 (1 H, NH), 6.2–8.0 (9 H, aromatic H's).

Poly(4,4′-diphenylamine benzylidene) (PDPAB, 3b). The reaction mixture was 10 g of diphenylamine, 6.27 g of benzaldehyde, 1.1 mL of 96% concentrated sulfuric acid, and 50 mL of *p*-dioxane. The reaction was maintained at 90 °C for 22 h. A yellowish-green reaction mixture was poured into 800 mL of stirring methanol, recovered by filtration, recrystallized from THF/hexane, and dried in a vacuum oven at 60 °C for 12 h. The product was a slightly green powder (80% yield). Anal. Calcd for $[(C_{19}H_{15}N)_{0.93}(C_{19}H_{16}NSO_4)_{0.07}]_n$: C, 86.40; N, 5.30; H, 5.75. Found: C, 86.31; H, 5.60; N, 5.20. IR (film on NaCl, cm^{-1}): 3386, 3050, 3013, 2971, 2865, 1602, 1511, 1450, 1386, 1312, 1249, 1245, 1199, 1178, 1168, 809, 747, 699. UV–vis (λ_{max}, THF): 297 nm (log ϵ = 4.36). ^{1}H NMR (δ, ppm, referenced to TMS, in DMSO-d_6): 5.30 (1 H, CH), 5.73 (1 H, NH), 6.40–7.30 (13 H, aromatic H's).

Poly(4,4′-diphenylamine *p*-nitrobenzylidene) (PDPANB, 3c). The reaction mixture was 5 g of diphenylamine, 5.6 g of *p*-nitrobenzaldehyde, 0.62 mL of 96% concentrated sulfuric acid, and 50 mL of *p*-dioxane. The reaction was maintained at 90 °C for 1 h. A yellow reaction mixture was poured into 600 mL of stirring methanol, recovered, recrystallized from THF/hexane, and dried in a vacuum oven at 70 °C for 10 h. The product was a yellow powder (70% yield). Anal. Calcd for $[(C_{19}H_{14}N_2O_2)_{0.94}(C_{19}H_{15}N_2SO_6)_{0.06}]_n$: C, 74.06; H, 4.58; N, 9.07. Found: C, 74.00; H, 4.48; N, 9.07. IR (film on NaCl, cm^{-1}): 3394, 3020, 2964, 2858, 1604, 1515, 1346, 1301, 1245, 1175, 1105, 1006, 809, 738, 689. UV–vis (λ_{max}, THF): 294 nm (log ϵ = 4.45). ^{1}H NMR (δ, ppm. referenced to TMS, in DMSO-d_6): 5.55 (1 H, CH), 6.00 (1 H, NH), 6.40–7.40 (10 H, aromatic H's), 8.10 (2 H, aromatic H's on the side group).

Poly(4,4′-diphenylamine *p*-(heptyloxy)benzylidene) (PDPAHB, 3d). The reaction mixture was 3.84 g of diphenylamine, 5 g of *p*-(heptyloxy)benzaldehyde, 40 mL of *p*-dioxane, and 0.41 mL of 96% sulfuric acid. The reaction was maintained at 85 °C for 24 h. A yellowish-green mixture was precipitated into 500 mL of stirring hexane, recovered, recrystallized from THF/hexane, and dried in a vacuum oven at 60 °C for 12 h. The product was a yellow but slightly green powder (68% yield). Anal. Calcd for $[C_{26}H_{29}NO)_{0.83}(C_{26}H_{30}NSO_5)_{0.17}]_n$: C, 80.48; H, 7.58; N, 3.61; O, 6.93. Found: C, 80.50; H, 7.44; N, 4.06; O, 7.16. IR (film on NaCl, cm^{-1}): 3323, 3056, 2929, 2858, 1603, 1509, 1463, 1315, 1244, 1175, 1112, 1020, 823, 745, 689. UV–vis (λ_{max}, CH_2Cl_2): 289 nm (log ϵ = 4.37). ^{1}H NMR (δ, ppm, referenced to TMS): 0.8 (3 H, CH_3), 1.3 (8 H, $(CH_2)_4$), 1.66 (2 H, CH_2), 3.85 (2 H, OCH_2), 5.28 (1 H, C(R)H), 5.66 (1 H, NH), 6.60–8.40 (12 H, aromatic H's).

Poly(4,4′-diphenylimine methine) (PDPIM, 4a). The reaction mixture was 1.28 g of PDPAM, 1.60 g of DDQ, and 60 mL of anhydrous NMP. The reaction mixture became dark purple immediately when DDQ was added into the reaction mixture. The reaction was maintained at 80 °C for 8 h. A dark purple reaction mixture was poured into 800 mL of stirring deionized water, recovered, extracted by acetone in a Soxhlet apparatus for 12 h, and dried in a vacuum oven at 70 °C for 12 h. The product was a dark purple powder (86% yield). The product was dissolved in NMP and only 40% of the product was soluble in NMP. Anal. Calcd for $[(C_{13}H_9N)_{0.98}(C_{13}H_{10}NSO_4)_{0.02}]_n$: C, 86.20; H, 5.00; N, 7.73. Found: C, 83.51; H, 5.61; N, 7.27. IR (film on NaCl, cm^{-1}): 1661, 1587, 1506, 1300, 1280, 1170, 921, 830, 759. UV–vis (λ_{max}, NMP): 378 nm (log ϵ = 4.06), 524 nm (log ϵ = 3.34). ^{1}H NMR (δ, ppm, referenced to TMS, soluble fraction in DMSO-d_6): 6.8–7.8 (10 H, =CH and aromatics H's).

Poly(4,4′-diphenylimine benzylidene) (PDPIB, 4b). The reaction mixture was 1.60 g of PDPAB, 1.41 g of DDQ, and 60 mL of NMP. The reaction mixture became dark green immediately after DDQ was added. The reaction was maintained at 80 °C for 6 h. A dark green reaction solution was poured into 600 mL of stirring deionized water, recovered, extracted by methanol and then acetone in a Soxhlet apparatus for 12 h, and dried in a vacuum oven at 70 °C for 24 h. The product was a dark green powder (86% yield). Anal. Calcd for $[(C_{19}H_{13}N)_{0.93}(C_{19}H_{16}NSO_4)_{0.07}]_n$: C, 87.07; H, 5.80; N, 5.34. Found: C, 85.58; N, 5.19; H, 5.23. IR (film on NaCl, cm^{-1}): 3048, 2940, 1669, 1577, 1507, 1449, 1375, 1341, 1165, 1119, 893, 815, 745, 696. UV–vis (λ_{max}, NMP): 301 nm (log ϵ = 4.55), 490 nm (log ϵ = 3.76). ^{1}H NMR (δ, ppm, referenced to TMS, in DMSO-d_6): 6.2–8.2 (13 H, aromatic H's).

Poly(4,4′-diphenylimine *p*-nitrobenzenylidene) (PDPINB, 4c). The reaction mixture was 2 g of PDPANB, 1.8 g of DDQ, and 60 mL of NMP. The reaction mixture became dark green immediately when DDQ was added. The reaction was maintained at 85 °C for 10 h. A dark green reaction mixture was poured into 600 mL of stirring deionized water, recovered, extracted by methanol in a Soxhlet apparatus for 12 h, and dried in a vacuum oven at 70 °C for 10 h. The product was a dark green powder (90% yield). Anal. Calcd for $[(C_{19}H_{12}N_2O_2)_{0.94}(C_{19}H_{13}N_2SO_6)_{0.06}]_n$: C, 74.55; H, 3.95; N, 9.15. Found: C, 72.94; H, 4.58; N, 8.89. FTIR (film on NaCl, cm^{-1}): 3267, 3020, 2928, 2858, 1668, 1600, 1575, 1517, 1400, 1346, 1165, 1104, 1013, 907, 836, 808, 745, 696. UV–vis (λ_{max}, NMP): 296 nm (log ϵ = 4.40), 541 nm (log ϵ = 3.22). ^{1}H NMR (δ, ppm, referenced to TMS, in DMSO-d_6): 7.00 (8 H, aromatic H's on the main chain), 7.50 (2 H, aromatic H's on the side chain), 8.14 (2 H, aromatic H's on the side chain).

Poly[4,4′-diphenylimine *p*-(heptyloxy)benzylidene] (PDPIHB, 4d). The reaction mixture was 2 g of PDPAHB, 0.86 g of DDQ, and 40 mL of anhydrous THF. The solution turned to dark blue immediately when DDQ was added into the reaction mixture. The reaction was maintained at 65 °C for 17 h. A dark blue reaction solution was poured into 500 mL of stirring hexane, recovered, recrystallized from THF/hexane, extracted by benzene in a Soxhlet apparatus for 12 h, and dried in a vacuum oven at 50 °C for 12 h. The product was a dark blue powder (70% yield). Anal. Calcd for $[(C_{26}H_{27}NO)_{0.83}(C_{26}H_{28}NSO_4)_{0.17}]_n$: C, 80.90; H, 7.31; N, 3.63; O, 6.96. Found: C, 78.68; H, 6.96; N, 3.79; O, 7.50. IR (film on NaCl, cm^{-1}): 3260, 3056, 2950, 2922, 2851, 1573, 1485, 1422, 1367, 1347, 1317, 1260, 1106, 1021, 992, 928, 837, 795, 753, 698. UV-vis (λ_{max}, CH_2Cl_2): 639 nm (log ϵ = 4.11), 501 nm (log ϵ = 3.90), 269 nm (log ϵ = 3.90). ^1H NMR (δ, ppm, referenced to TMS in DMSO-d_6): 0.80 (3 H, CH_3), 1.30 (8 H, $(CH_2)_4$), 1.66 (2 H, CH_2), 3.91–4.14 (2 H, OCH_2), 6.60–7.60 (12 H, aromatic H's).

Characterization. Infrared spectra of polymer thin films were recorded on a NaCl window at room temperature using a Nicolet Model 20 SXC FTIR spectrometer. The ^1H NMR spectra were obtained by using a General Electric Model QE300 instrument. Elemental analysis was done by Galbraith Laboratories, Inc. (Knoxville, TN), and Oneida Research Services, Inc. (Whitesboro, NY).

The molecular weight distribution of PDPAB, PDPANB, and PDPAHB was measured in a size-exclusion chromatograph constructed with a HPLC metering pump (Constametric III, Milton Roy), two PL gel columns in series (500 and 10 000 Å, Hewlett Packard) housed in a column oven (Jones Chromatography), and an absorbance detector (V^4 Absorbance detector, ISCO) set at 254 nm. The gel permeation chromatograph (GPC) was operated in THF at 40 °C. The intrinsic viscosities, $[\eta]$, of all polymers in DMF or NMP were determined at 30 °C by using a Cannon-Ubbelohde capillary viscometer and a constant-temperature bath. The intrinsic viscosity values were extracted from the intersection of plots of the reduced viscosity (η_{sp}/C) and inherent viscosity ($\eta_{inh} = [\ln \eta_{rel}]/C$) versus solution concentration.

Electron spin resonance (ESR) spectra were recorded on a Bruker EP 300 spectrophotometer equipped with a dual microwave cavity. Diphenylpicrylhydrazyl (DPPH) was used as a reference for determination of *g*-values. The standard solution of 4-hydroxy-2,2,6,6-tetramethylpiperidinyloxy (4-hydroxy-TEMPO) in THF was used in the determination of spin concentrations. The concentration of the standard solution was 3.998×10^{-4} M. The experiments were performed at room temperature. ESR samples (5–10 mg) were prepared in quartz sample tubes in a drybox under a nitrogen atmosphere. The preparation of the ESR sample for the study of the mechanism of the dehydrogenation reaction on the precursor polymer PDPAHB is described below. A total of 33 mg of PDPAHB was dissolved in 0.3 g of THF. This solution was poured into 15 mg of DDQ in an 8-mL vial. This mixture was shaken for a few seconds, and then 0.3 mL of the mixture was placed into a quartz sample tube. The quartz sample tube was sealed using parafilm and then put in an oven at 60 °C under a nitrogen atmosphere. The ESR spectra of this mixture were recorded with time and under the same experimental conditions (the time constant, modulus amplitude, and receiver gain were kept the same), and a standard solution was used to determine the spin concentration.

Thermal analysis, differential scanning calorimetry (DSC), and thermogravimetric analysis (TGA) were done using a Du Pont Model 1090B thermal analyzer or a Du Pont Model 2100 thermal analyst system based an IBM PS/2 Model 60 computer and using flowing nitrogen. Indium (156.4 °C) standard was used to calibrate the accuracy of the measured transition points. Samples were sealed in DSC pans and run at 20 °C/min. TGA runs were performed at a heating rate of 10 °C/min. Electronic absorption spectra were obtained at room temperature in the range of 185–3200-nm wavelength using a Perkin-Elmer Lambda 9 UV-VIS-near-IR spectrophotometer. Thin films were cast from a 2–3 wt % solution by spin coating at a speed of 4000 rpm for 1 min.

Scheme I

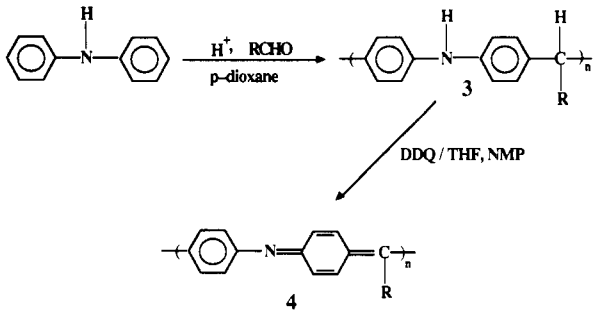

Results and Discussion

Polymerization and Dehydrogenation. Poly(4,4′-diphenylamine methylenes) (**3** in Chart I) which are analogues of the leucoemeraldine form of polyaniline were synthesized from diphenylamine and aldehydes under acid catalysis as shown in Scheme I. A linear polymer chain whose structure will be subsequently discussed in detail can be expected on mechanistic grounds. The protonated aldehyde electrophile can attack diphenylamine at the ortho or para position of the benzene ring because the amino group is an ortho/para director under electrophilic aromatic substitution. However, the para position is favored in a polymerization reaction because the strong steric hindrance at the ortho position would hinder chain growth. Related *p*-phenylene-linked polyaniline derivatives have previously been prepared from diphenylamine,[21] *N*-alkyldiphenylamine,[22] and 3-alkoxydiphenylamine[20] by chemical and electrochemical polymerizations. Our evidence for the linear chain structure of the present polymers includes infrared and NMR spectra and solubility of the polymers in organic solvents, as will be discussed in detail below. Since this polymerization is catalyzed by protonic acid (H_2SO_4), a common way to terminate the propagation of the growing polymer chain is the reaction of the propagating cation with the counterion (HSO_4^-). Thus, these polymers may be expected to have HSO_4 end groups.

The poly(4,4′-diphenylimine methines) (**4** in Chart I) which are analogues of the polypernigraniline base or poly(*p*-phenyleneimine) (**2**) were prepared by exhaustive dehydrogenation of the corresponding poly(4,4′-diphenylamine methylenes) with 2,3-dichloro-5,6-dicyano-1,4-benzoquinone. Although the oxidation of polymers **3** with DDQ could in principle be carefully controlled in order to produce polymers with oxidation states between the fully reduced **3** and fully oxidized **4** similar to the parent polyaniline, our initial objective was to obtain the completely oxidized form for comparison with pernigraniline. Therefore, excess DDQ was used in the dehydrogenation reactions in order to effect complete oxidation of polymers **3**. Achievement of the fully oxidized polymers **4** was confirmed by characterization of their structures and properties.

Electron spin resonance spectroscopy was used to probe the possible intermediates of the polymer dehydrogenation reactions with DDQ. Dehydrogenation reactions with DDQ are generally ionic reactions.[23,24] However, radical intermediates are also known in some cases. The conversion of perinaphthene to perinaphthyl by DDQ has been proposed to be a radical reaction.[25] The dehydrogenation of bilirubin to biliverdin with DDQ was also shown to be via a radical intermediate.[26] Solution samples of PDPAHB (**3d**) and DDQ separately do not show any ESR signal. However, when mixed, the PDPAHB/DDQ solution exhibits a strong ESR signal. A typical ESR spectrum of a PDPAHB/DDQ reaction mixture is shown in Figure

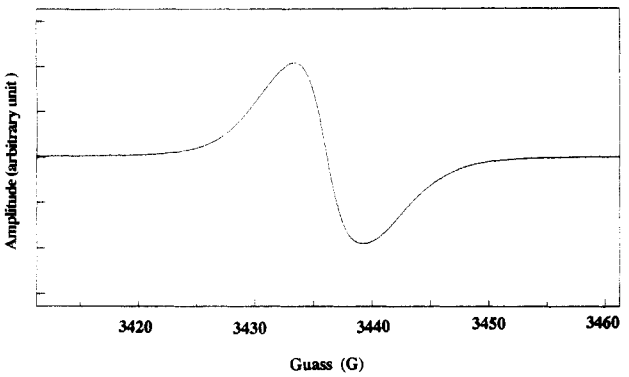

Figure 1. ESR spectrum of a PDPAHB/DDQ solution.

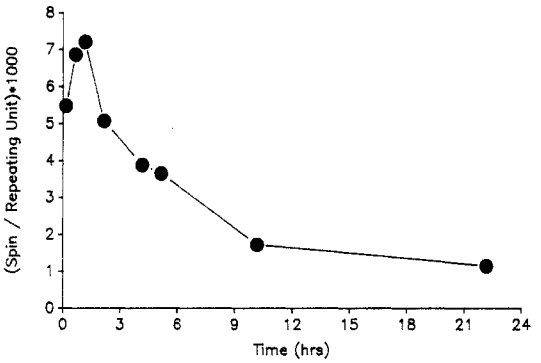

Figure 2. Time dependence of the spin concentration of a PDPAHB/DDQ solution.

1. ESR spectra of the polymer/DDQ reaction solution were taken with time as a way of following the dehydrogenation reaction. The *g*-value of the ESR signals was between 2.004 36 and 2.005 44, and the line width was from 4.9 to 10.1 G. The *g*-values are about 0.003 larger than that of a free electron (2.002 32) and hence indicate the radical to be on the nitrogen atom of the polymer and/or the oxygen atom of DDQ. Figure 2 shows the spin concentration of the PDPAHB/DDQ solution with time. The spin concentration increased rapidly with time, reaching a maximum of 1.19×10^{19} spin/g within about 1.2 h, and then gradually decreased by an order of magnitude within 10 h. These results clearly indicate that radical species are the reaction intermediates when polymers **3** are oxidized with DDQ.

Of the eight pure polymers prepared only one, PDPIM (**4a**), showed an ESR signal. The ESR signal of PDPIM has a *g*-value of 2.005 44 and a line width of 5.67 G and corresponds to about 1 spin per 3851 repeat units or 8.56×10^{17} spin/g. The spin concentration of PDPIM is comparable to or smaller than that reported for conjugated polymers such as *trans*-polyacetylene (10^{19} spin/g),[1c] poly(*p*-phenylene) (10^{19} spin/g),[1c] polypyrrole (6×10^{19} spin/g),[27] polythiophene (3.3×10^{17} spin/g),[1c] and poly(*p*-phenylenevinylene) (5.9×10^{17} spin/g).[28]

Polymer Structure. The proposed structures of polymers **3** and **4** (Chart I) were confirmed by spectroscopy (FTIR, ^{1}H NMR, UV–Vis), elemental analysis, and other physical properties of the polymers. Figure 3 shows the FTIR absorption spectra of the basic polymer **3a** (PDPAM) and its fully oxidized conjugated derivative **4a** (PDPIM). The para linkage of the polymers is identified from two regions of the FTIR spectra. The strong band at 809 cm^{-1} in PDPAM is characteristic of the C–H out-of-plane bending of the 1,4-disubstituted benzene ring. The two bands at 1886 and 1766 cm^{-1} in the spectrum of PDPAM are identical with the reported characteristic bands of the 1,4-disubstituted benzene ring.[29] The N–H stretching

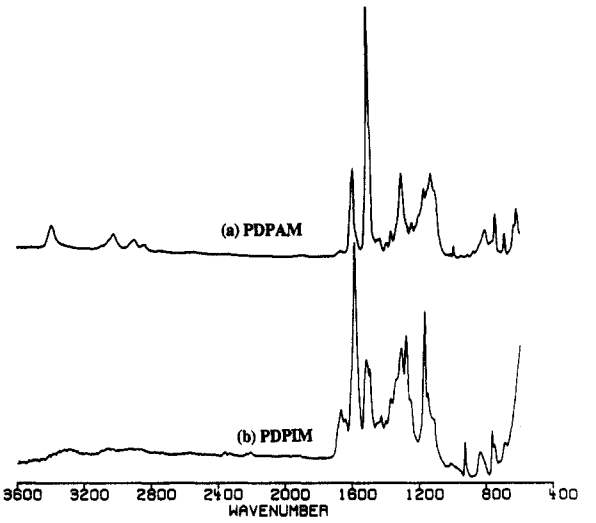

Figure 3. FTIR absorption spectra of PDPAM (a) and PDPIM (b).

Table I
Assignments of the FTIR Spectra of Poly(4,4′-diphenylamine methylenes) and Poly(4,4′-diphenylimine methines) (All Units in cm^{-1})

polymer	out-of-plane C–H bending	N–H stretching	CH_2 or CHR stretching	C–C ring stretching	C=N stretching
PDPAM	809	3394	2837, 2900	1512, 1597	
PDPAB	809	3386	2865, 2971	1511, 1602	
PDPANB	809	3394	2858, 2964	1514, 1604	
PDPAHB	823	3323	2858, 2929	1508, 1603	
PDPIM	830			1506, 1587	1587
PDPIB	815			1495, 1576	1576
PDPINB	808–836			1510, 1600	1575
PDPIHB	837			1573	1573

vibration band of PDPAM is observed at 3394 cm^{-1}. The aliphatic C–H stretching bands of PDPAM are observed in the region 2837–2900 cm^{-1}. The band at 1310 cm^{-1} in PDPAM is assigned to the C–N stretching. Similar assignments of the FTIR spectra of **3b** (PDPAB), **3c** (PDPANB), and **3d** (PDPAHB) are collected in Table I.

Major changes are observed in the FTIR spectra when the fully reduced polymers **3** are converted to the fully oxidized forms **4**. For example, as seen in Figure 3, the characteristic N–H stretching band at 3394 cm^{-1} in PDPAM has completely disappeared in PDPIM (**4a**). Similarly, the aliphatic CH_2 stretching vibration bands in PDPAM at 2837 and 2900 cm^{-1} have also been completely eliminated after dehydrogenation to PDPIM. Furthermore, the intensity of the peaks at around 1510 and 1600 cm^{-1} has also been dramatically changed. The increased intensity of the band near 1575 cm^{-1} and corresponding decrease of the C–N stretching band at 1310 cm^{-1} confirm the transformation of the C–N bond in the polymers to a C=N bond by the dehydrogenation. A similar change in intensity is observed in pernigraniline and a fully oxidized aniline oligomer compared to the emeraldine base form of polyaniline.[9,30,31] A new band near 1660 cm^{-1} in polymers **4** is due to C=C stretching originating from methine carbon. Assignments of characteristic FTIR bands in polymers **4a–d** are also given in Table I.

Figure 4 shows the ^{1}H NMR spectra of PDPAM and its fully oxidized conjugated derivative in DMSO-d_6 solvent. The strong peak at 3.4 ppm in both spectra is due to water in the solvent. A characteristic feature of the NMR spectra of the fully reduced polymers **3** is the bridge methylene hydrogen resonance, –C(R)H–, which is a singlet resonance at 3.71 ppm in **3a**, 5.30 ppm in **3b**, 5.66 ppm in **3c**, and 5.28 ppm in **3d**. The downfield shift of this resonance in **3c** (PDPANB) is due to the strong electron-withdrawing NO_2

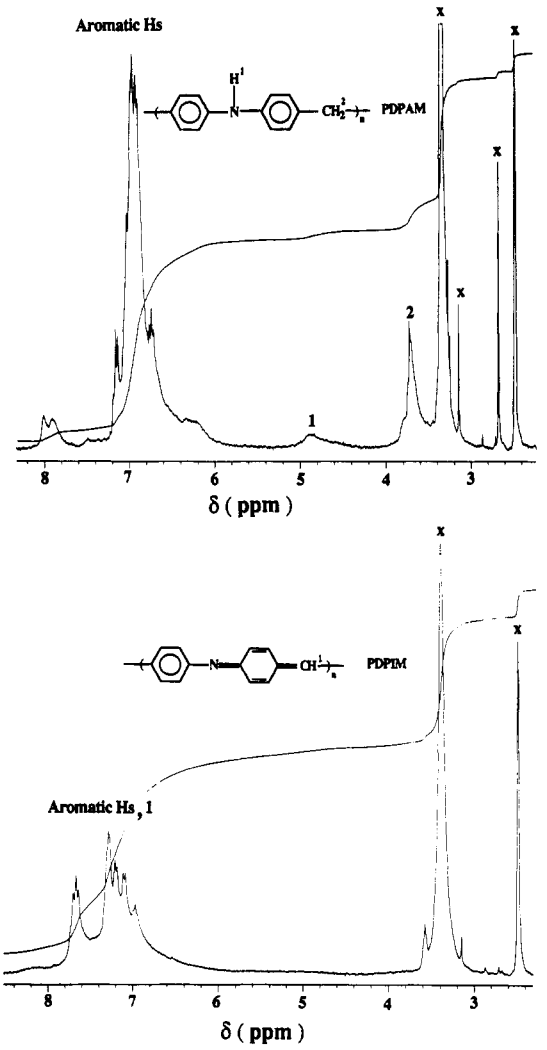

Figure 4. ^{1}H NMR spectra of PDPAM (a) and PDPIM (b). ×'s indicate DMSO-d_6 or water contained in DMSO-d_6.

group. The amine (N–H) hydrogen resonance in polymers **3a–d** was a singlet at 4.88, 5.72, 6.00, and 5.66 ppm, respectively. The aromatic hydrogens in polymers 3 gave overlapping resonances in the region 6–8 ppm as expected. The number of protons corresponding to each resonance determined from integration of the peaks was in good agreement with the proposed structures. The only exception was the N–H resonance whose integration was not always very accurate due to the broadness of the resonance which arises from the slow rate of exchange of the proton on the nitrogen.[32]

Oxidation of PDPAM by DDQ to PDPIM results in major changes in the NMR spectrum as observed in Figure 4. For example, the methylene hydrogen and amine hydrogen resonances at 3.71 and 4.88 ppm, respectively, in PDPAM have completely disappeared in PDPIM. Another significant change is the large downfield shift of the benzene hydrogen resonances of PDPIM compared to PDPAM. This shift can be explained by the larger π-electron delocalization of the polymer backbone after dehydrogenation; such an electronic delocalization would induce a magnetic field against the applied field and thus result in a downfield shift of the ring hydrogen resonances.

The results of the elemental analysis of the polymers were in fair agreement with the proposed structures. Since the molecular weights of these polymers are low (<10 000), it was necessary to take the effects of end groups such as HSO_4 into account to get good agreement in the elemental analysis. The elemental analysis results were also used to estimate the molecular weights of the polymers for comparison with GPC data.

Table II
Intrinsic Viscosities [η], T_g, and Molecular Weights of Polyaniline Derivatives

polymer	[η] (dL/g)[a]	T_g (°C)	$\bar{M}_n$[b]	$\bar{M}_w$[c]	$\bar{M}_n$[c]
PDPAM	0.18[d]	143	9160		
PDPAB	0.11	110	4500	6500	3300
PDPANB	0.12		5200	8300	4700
PDPAHB	0.05	81	2100	3500	2500
PDPIM	0.19[d]				
PDPIB	0.17				
PDPINB	0.13				
PDPIHB	0.07	175			

[a] In NMP solvent. [b] Estimated from elemental analysis. [c] $\bar{M}_w$ and $\bar{M}_n$ determined by gel permeation chromatography. [d] NMP-soluble fraction: PDPAM was 70% soluble in NMP; PDPIM was 40% soluble in NMP.

Solution Properties and Molecular Weight. The fully reduced polymers were generally soluble in organic solvents including THF, DMF, DMSO, and NMP except PDPAM (**3a**) which was only partially (70%) soluble in NMP, DMF, and DMSO. As expected, the fully oxidized polymers were less soluble in organic solvents than their corresponding fully reduced forms, owing to the increased stiffness of the chains of polymers **4**. PDPIM (**4a**) is only 40% soluble in NMP or DMF. PDPIB (**4b**) and PDPINB (**4c**) are completely soluble in NMP and DMF but only partially soluble in THF. PDPIHB (**4d**) is completely soluble in all of the above organic solvents due to its long alkoxy side group. The NMP-insoluble fractions of PDPAM and PDPIM are most likely the higher molecular weight fractions of these polymers. This was partly confirmed by the fact that the NMP-insoluble fraction of PDPIM was partially soluble in sulfuric acid and $GaCl_3$/nitromethane in which the polyemeraldine base and polypernigraniline base were found to be completely soluble.[6] Incomplete solubility of PDPIM in either sulfuric acid or $GaCl_3$/nitromethane is probably due to the reduction of the imine nitrogen sites available for protonation (H_2SO_4) or complexation ($GaCl_3$/nitromethane) compared to the all-nitrogen polyanilines.

The molecular weight and molecular weight dispersity of the polymers were investigated by elemental analysis, gel permeation chromatography (GPC), and intrinsic viscosity measurement. The estimated number-average molecular weight ($\bar{M}_n$) of the fully reduced polymers is shown in Table II and was between 2100 and 9160. This corresponds to 50 repeat units or 100 rings in the case of PDPAM. The degree of polymerization was only about 7–16 for the remaining three polymers. From the weight-average ($\bar{M}_w$) and number-average ($\bar{M}_n$) molecular weights estimated from GPC, the dispersity ($\bar{M}_w/\bar{M}_n$) was 1.97, 1.77, and 1.4 respectively for PDPAB, PDPANB, and PDPAHB. The intrinsic viscosities [η] of all eight polymers are shown in Table II; the [η] values were in the range of 0.05–0.19 dL/g. The slight increase of the intrinsic viscosity of the oxidized polymers compared to the reduced polymers is due to the greater stiffness of the oxidized polymer chains.

Thermal Properties. The thermal stability of this class of polymers is shown in the TGA thermograms of representative members, PDPAM, PDPIM, PDPAHB, and PDPIHB, in Figure 5. The onset of thermal decomposition in nitrogen is relatively high (~480 °C) in the two basic polymers without side-group substitution at the bridge carbon (PDPAM, PDPIM). As expected the polymers with the longest side group (PDPAHB, PDPIHB) exhibited the least thermal stability as shown by their

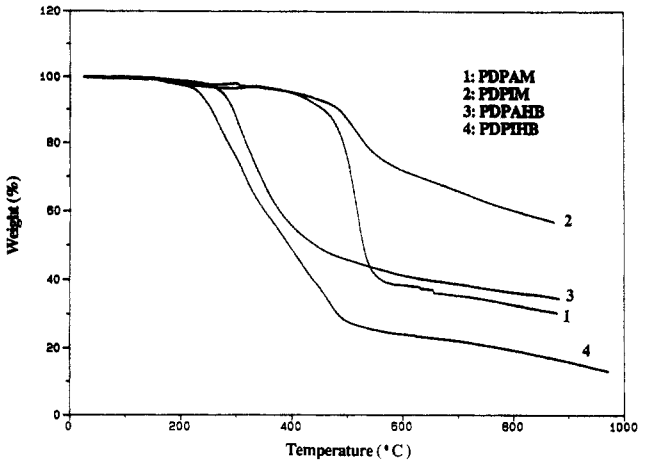

Figure 5. TGA thermograms of PDPAM (1), PDPIM (2), PDPAHB (3), and PDPIHB (4) in flowing nitrogen at a heating rate of 10 °C/min.

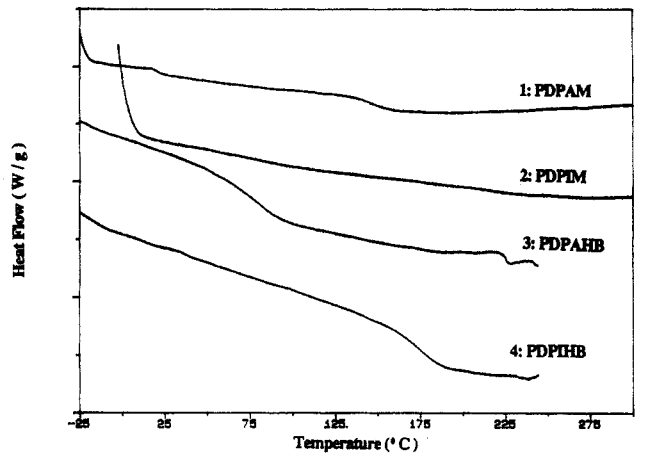

Figure 6. DSC thermograms of PDPAM (1), PDPIM (2), PDPAHB (3), and PDPIHB (4) at a heating rate of 20 °C/min.

onset of thermal decomposition in nitrogen of ~275 °C. It is interesting that the fully oxidized polymers have a slightly better thermal stability than the fully reduced forms.

Figure 6 shows the DSC thermograms of four of the polymers in flowing nitrogen at a heating of 20 °C/min. Of the eight polymers, the glass transition temperature (T_g) could be determined from the DSC scans for only four. The T_g values were in the range 81–175 °C as shown in Table II. The T_g is clearly reduced when a side group is substituted at the methylene or methine carbon. The DSC results also provide additional evidence that the chain stiffness increases with dehydrogenation or oxidation. For example, the T_g of PDPIHB is more than twice the T_g of its corresponding fully reduced form (PDPAHB). The glass transition had significantly increased that it could not be determined in the case of PDPIM, PDPINB, and PDPIB.

Optical Properties. The solution optical absorption spectra of the four fully reduced polymers **3** are shown in Figure 7. All the polymers exhibit a strong absorption with a maximum (λ_{max}) near 295 nm (4.2 eV). This absorption band is assigned to the π–π^* optical band-gap transition. The donor and acceptor side groups at the bridge methylene carbon have a negligible effect on the electronic structure and optical properties of the fully reduced polymers. A comparison of the absorption spectrum of PDPAM (**3a**) with that of the polyleucoemeraldine base (PLEMB, 1), as done in Figure 8, shows a significant difference between the two. The λ_{max} of

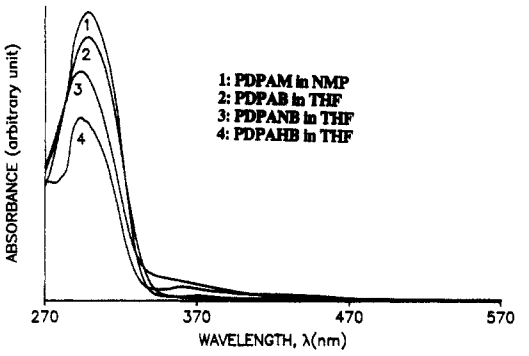

Figure 7. Electronic absorption spectra of PDPAM (1, in NMP), PDPAB (2, in THF), PDPANB (3, in THF), and PDPAHB (4, in THF).

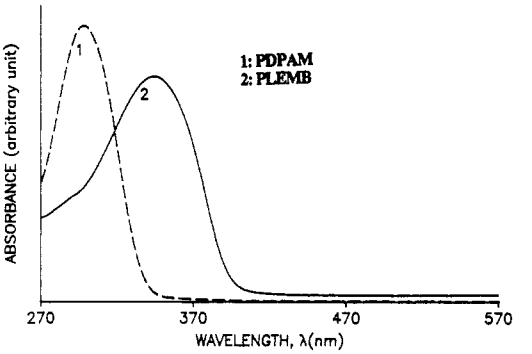

Figure 8. Solution optical absorption spectra of PDPAM and the polyleucoemeraldine base (PLEMB) in NMP.

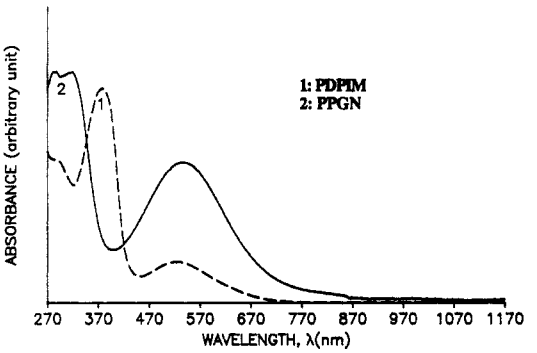

Figure 9. Solution optical absorption spectra of PDPIM and the polypernigraniline base (PPGN) in DMF.

PDPAM is blue shifted from that of PLEMB (λ_{max} = 334 nm, 3.71 eV). The origin of the relatively small energy of the π–π^* transition in PLEMB is due to the significant delocalization of the electron pair on amine nitrogen atoms to the adjacent benzene rings. Hence, it is not surprising that the energy of the π–π^* optical gap is significantly increased with a 50% reduction of the nitrogen atoms.

The solution optical absorption spectrum of PDPIM (**4a**) is shown along with that of the polypernigraniline base (PPGN) in Figure 9. The two electronic spectra in Figure 9 are very similar in structure although there are very important differences. The optical absorption spectrum of a thin film of PDPIM which is shown in Figure 9 exhibits absorption maxima at 254 nm (4.88 eV), 374 nm (3.32 eV), and 540 nm (2.3 eV). These transitions correspond to transitions at 4.6, 3.8, and 2.2 eV reported for polypernigraniline.[30,31] There is a general agreement that the UV transitions in polypernigraniline are due to π–π^* transitions.[12,13] Although theoretical calculations have suggested the visible band at 2.2 eV in PPGN to be due to a π–π^* optical bandgap transition, other possibilities that have been considered include a molecular "exciton"

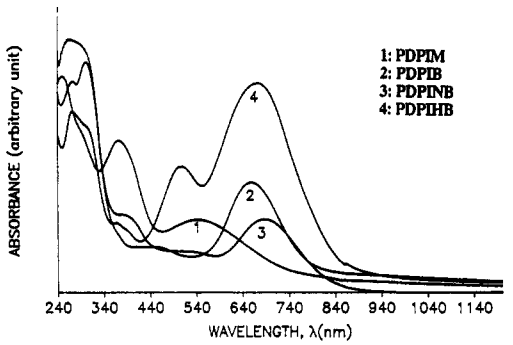

Figure 10. Electronic absorption spectra of PDPIM (1), PDPIB (2), PDPINB (3), and PDPIHB (4) films on fused silica substrates.

Table III
Optical Properties of Poly(4,4′-diphenylimine methine) Solutions and Films

polymer	λ_{max}(solution)[a] (nm)	λ_{max}(film) (nm)	E_g (film) (nm) [eV]
PDPIM	379, 525	251, 374, 540	750 [1.65]
PDPIB	301, 489	302, 660	800 [1.55]
PDPINB	296, 541	263, 687	830 [1.49]
PDPIHB	296, 488, 293,[b] 493,[b] 639,[b] 269,[c] 501,[c] 633[c]	271, 507, 671	850 [1.46]

[a]In NMP. [b]In THF. [c]In CH_2Cl_2.

transition[33] or an n–π^* transition.[34] The calculated band gap (E_g) for PPGN is 1.4 eV and is to be compared to the energy of the optical absorption edge rather than the peak of the absorption. The positions of the optical transitions in PDPIM are very close to those in PPGN so that we can assume that they originate from similar electronic states. The most important effect of the imine nitrogen atom on the electronic structure of PPGN is the larger oscillator strength of the 2.2-eV absorption band (absorption coefficient = 2.8×10^4 cm^{-1}) compared to the same band in PDPIM (absorption coefficient = 1.7×10^4 cm^{-1}). Although such a reduction in the transition dipole moment of the visible absorption band on 50% reduction of the imine nitrogen atoms would be consistent with an n–π^* transition, we believe that the visible absorption band near 2.2 eV in both PPGN and PDPIM is still best explained by a π–π^* optical band-gap transition.

Figure 10 shows the optical absorption spectra of thin films of the four fully oxidized polymers 4 (PDPIM, PDPIB, PDPINB, and PDPIHB). The corresponding solution spectra in either NMP or THF were nearly identical to those in Figure 10. The λ_{max} of the solution and thin film spectra and an optical band gap (E_g) defined as the energy of absorption edge in thin films are shown in Table III. Unlike the fully reduced polymers 3 in which the side group has no effect, we clearly see in Figure 10 and Table III that the side group has a dramatic effect on the electronic structure of the fully oxidized polymers 4. There is a dramatic change in both the position and the oscillator strength of the visible absorption band near 2.2 eV depending on the substituent at the methine carbon atom. For example, the λ_{max} of PDPIM film (540 nm, 2.3 eV) is dramatically increased to 687 nm (1.80 eV) in the electron-withdrawing *p*-nitrophenyl-substituted polymer (PDPINB). The strong sensitivity of the energy and oscillator strength of the visible absorption band in these fully oxidized polymers to the substituent (R) at the methine carbon (=C(R)) suggests that the transition is due to π-electron delocalization along the polymer backbone. Thus, these results confirm that the origin of the 2-eV transition in PDPIM and PPGN is due to a π–π^* optical band-gap transition.

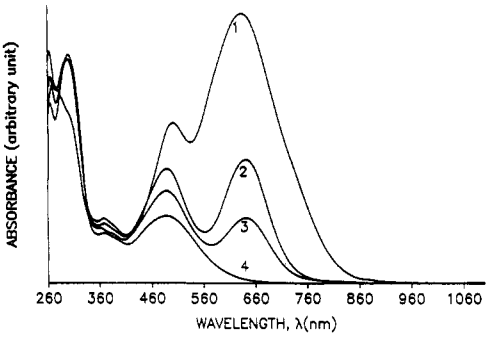

Figure 11. Electronic absorption spectra of PDPIHB in different volume ratios of NMP and CH_2Cl_2 mixed solvent: (1) pure CH_2Cl_2; (2) CH_2Cl_2:NMP = 5:1; (3) CH_2Cl_2:NMP = 5:1.5; (4) pure NMP.

The optical properties of conjugated polymers **4b** (PDPIB), **4c** (PDPINB), and **4d** (PDPIHB) were found to exhibit various effects of chromism. The polymers in solution exhibit solvatochromism. In dilute solutions at concentrations in the range 10^{-5}–2×10^{-3} M, solutions of PDPIHB in NMP or DMF are red but are dark blue in THF or CH_2Cl_2. Figure 11 shows the solution optical absorption spectra of PDPIHB in different ratios of CH_2Cl_2 to NMP. The optical spectra show that the gradual color changes are controlled by the "quality" or nature of the solvent. On gradual addition of NMP to a solution of PDPIHB in CH_2Cl_2, the color changes gradually from blue to red and vice versa. Similar solvatochromism was observed in PDPIB and PDPINB. However, at high concentrations ($>2 \times 10^{-3}$ M) solutions of PDPIB and PDPIHB in NMP were dark blue whereas PDPINB in NMP remained red. Thin films cast from even the red NMP or DMF solutions were in all cases blue or green. These results on the chromism of polypernigraniline derivatives (4) can be explained by *intrachain* conformational changes of the polymer backbone in the different solvent environment. A similar, though not as dramatic, solvatochromism has been reported[17] in sulfonated polyemeraldine base where the 2.2-eV band in a water solution was shifted to 2.0 eV when NMP was added. Our observation of color changes at high concentration ($>2 \times 10^{-3}$ M) or when films were cast from a solution is explained by strong *interchain interactions* that result in aggregation of the chains. Similar effects of chromism in the solution- and solid-state optical properties of other conjugated polymers, most notably polydiacetylenes[35] and poly(3-hexylthiophene)[36] are well-known and have been explained by a similar mechanism.

Conclusions

We have synthesized several members of the fully reduced and the fully oxidized forms of a new family of polyaniline derivatives as polymer model systems for understanding the electronic structure, physical properties, and structure–property relationships in polyanilines and related ring-containing conjugated polymers. The fully reduced poly(4,4′-diphenylamine methylenes) in which an amine nitrogen atom alternates with a methylene carbon atom and *p*-phenylene rings were found to be air stable and to have a larger π–π^* optical band-gap transition energy than the polyleucoemeraldine base. The fully oxidized poly(4,4′-diphenylimine methines), on the other hand, have a π–π^* optical band-gap transition that varies from 540 nm (2.3 eV) to 687 nm (1.8 eV) depending on the side-group substitution at the methine carbon. The present results provide a new evidence for the view that the 2.2-eV transition in polypernigraniline originates from

a π–π^* interband transition. The conjugated polyaniline derivatives with a side-group substitution at the methine carbon were found to exhibit dramatic effects of chromism in solution or thin films; for example, **3d** is red in NMP and deep blue in THF or CH_2Cl_2. The preparation, electronic structure, and properties of related polymers with oxidation states between **3** and **4** and especially analogues of the polyemeraldine base are currently under investigation.

Acknowledgment. We thank John Osaheni for helpful discussion. This research was supported by the National Science Foundation (Grant CHE-912-0001) and Amoco Foundation.

References and Notes

(1) (a) Bredas, J. L., Chance, R. R., Eds. *Conjugated Polymeric Materials: Opportunities in Electronics, Optoelectronics, and Molecular Electronics*; Kluwer Academic Publishers: Dordrecht, Holland, 1990. (b) Fromer, J. E.; Chance, R. R. *Encl. Polym. Sci. Eng.* **1985**, 462–507. (c) Skotheim, T. A., Ed. *Handbook of Conducting Polymers*; Marcel Dekker: New York, 1986.

(2) (a) Heeger, A. J.; Orenstein, J.; Ulrich, D. R. *Nonlinear Optical Properties of Polymers*; Materials Research Society Proceeding; Materials Research Society: Pittsburgh, PA, 1988; Vol. 109. (b) Prasad, P. N., Ulrich, D. R., Eds. *Nonlinear Optical and Electroactive Polymers*; Plenum: New York, 1988. (c) Chemla, D. S.; Zyss, J. *Nonlinear Optical Properties of Organic Molecules and Crystals*; Academic Press: New York, 1987; Vols. 1 and 2. (d) Messier, J., Kajzar, F., Prasad, P. N., Ulrich, D. R., Eds. *Nonlinear Optical Effects in Organic Polymers*; Kluwer Academic Publishers: Dordrecht, Holland, 1989.

(3) MacDiarmid, A. G.; Chiang, J. C.; Halpern, M.; Mu, W. L.; Somasiri, N. L. D. *Synth. Met.* **1986**, *13*, 193–205.

(4) Nguyen, M. T.; Dao, L. H. *J. Electrochem. Soc.* **1989**, *136*, 2131–2132.

(5) MacDiarmid, A. G.; Mu, S. L.; Somasiri, N. L. D.; Wu, W. *Mol. Cryst. Liq. Cryst.* **1985**, *121*, 187–190.

(6) (a) Osaheni, J. A.; Jenekhe, S. A.; Vanherzeele, H.; Meth, J. S. *Chem. Mater.* **1991**, *3*, 218–221. (b) Osaheni, J. A.; Jenekhe, S. A.; Vanherzeele, H.; Meth, J. S.; Sun, Y.; MadDiarmid, A. G. *J. Phys. Chem.* **1992**, *96*, 2830–2836.

(7) Stafstrom, S.; Bredas, J. L.; Epstein, A. J.; Woo, H. S.; Tanner, D. B.; Huang, W. S.; MacDiarmid, A. G. *Phys. Rev. Lett.* **1987**, *59*, 1464–1467.

(8) Cao, Y.; Andreatta, A.; Heeger, A. J.; Smith, P. *Polymer* **1989**, *30*, 2305–2311.

(9) Epstein, A. J.; Ginder, J. M.; Zuo, F.; Bigelow, R. W.; Woo, H. S.; Tanner, D. B.; Richter, A. F.; Huang, W. S.; MacDiarmid, A. G. *Synth. Met.* **1987**, *18*, 303–309.

(10) Chiang, J. C.; MacDiarmid, A. G. *Synth. Met.* **1986**, *13*, 193–205.

(11) Boudreaux, D. S.; Chance, R. R.; Wolf, J. F.; Shacklette, L. W.; Bredas, J. L.; Themans, B.; Andre, J. M.; Silbey, R. *J. Chem. Phys.* **1986**, *85*, 4584–4590.

(12) dos Santos, M. S.; Bredas, J. L. *Phys. Rev. Lett.* **1989**, *62*, 2499–2502.

(13) Ginder, J. M.; Epstein, A. J. *Phys. Rev. Lett.* **1990**, *64*, 1184–1185.

(14) Leclerc, M.; Guay, J.; Dao, L. H. *Macromolecules* **1989**, *22*, 649–653.

(15) Dao, L. H.; Guay, J.; Leclerc, M.; Chevalier, J. W. *Synth. Met.* **1989**, *29*, E377–E382.

(16) Dao, L. H.; Guay, J.; Leclerc, M. *Synth. Met.* **1989**, *29*, E383–E388.

(17) Yue, J.; Wang, Z. H.; Cromack, K. R.; Epstein, A. J.; MacDiarmid, A. G. *J. Am. Chem. Soc.* **1991**, *113*, 2665–2671.

(18) Manohar, S. K.; MacDiarmid, A. G.; Cromack, K. R.; Ginder, J. M.; Epstein, A. J. *Synth. Met.* **1989**, *29*, E349–E356.

(19) Chevalier, J. W.; Bergeron, J. Y.; Dao, L. H. *Polym. Commun.* **1989**, *30*, 308–310.

(20) Guay, J.; Leclerc, M.; Dao, L. H. *J. Electroanal. Chem.* **1989**, *274*, 135–142.

(21) Guay, J.; Paynter, R.; Dao, L. H. *Macromolecules* **1990**, *23*, 3598–3605.

(22) Nguyen, M. T.; Dao, L. H. *J. Chem. Soc.*, Chem. *Commun.* **1990**, 1221–1222.

(23) Wakler, D.; Hiebert, J. D. *Chem. Rev.* **1967**, 153–195.

(24) Becker, H.-D.; Turner, A. B. In *The Chemistry of Quinonoid Compounds*; Patai, S., et al., Eds.; John Wiley & Sons: New York, 1988; Vol. 2, pp 1351–1384.

(25) Reid, D. H.; Fraser, M.; Molloy, B. B.; Payne, H. A. S.; Sutherland, R. G. *Tetrahedron Lett.* **1961**, 530–535.

(26) Mcdonagh, A. F.; Plama, L. A. *Biochem. J.* **1980**, *189*, 193–208.

(27) Scott, J. C.; Pfluger, P.; Krounbi, M. T.; Street, G. B. *Phys. Rev.* **1983**, *28*, 2140–2145.

(28) Gourley, K. D.; Lillya, C. P.; Reynolds, J. R.; Chien, J. C. W. *Macromolecules* **1984**, *17*, 1025–1033.

(29) Dyer, J. R. *Applications of Absorption Spectroscopy of Organic Compounds*; Prentice-Hall: Englewood Cliffs, NJ, 1965.

(30) Cao, Y. *Synth. Met.* **1990**, *35*, 319–332.

(31) Sun, Y.; MacDiarmid, A. G.; Epstein, A. J. *J. Chem. Soc., Chem. Commun.* **1990**, 529–531.

(32) Silverstein, R. M.; Blassler, G. C.; Morrill, T. C. *Spectrometric Identification of Organic Compounds*, 4th ed.; Wiley: New York, 1981.

(33) Duke, C. B.; Conwell, E. M.; Paton, A. *Chem. Phys. Lett.* **1986**, *131*, 82–86.

(34) Kim, Y. H.; Foster, C.; Chiang, J.; Heeger, A. J. *Synth. Met.* **1989**, *29*, E285–E290.

(35) Patel, G. C.; Chance, R. R.; Witt, J. D. *J. Chem. Phys.* **1979**, *70*, 4387–4392.

(36) Rughooputh, S. D. D. V.; Hotta, S.; Heeger, A. J.; Wudl, F. *J. Polym. Sci., Polym. Phys. Ed.* **1987**, *25*, 1071–1078.

Registry No. **3a** (copolymer), 120515-37-9; **3a** (SRU), 143330-81-8; **3b** (copolymer), 143330-75-0; **3b** (SRU), 143330-82-9; **3c** (copolymer), 143330-76-1; **3c** (SRU), 143330-83-0; **3d** (copolymer), 143330-77-2; **3d** (SRU), 143330-84-1; DDQ, 84-58-2.